Rev. Mexicana Astron. Astrof., 5, 79-85 (1981).

INTERNAL MOTIONS IN H II REGIONS. IX. THE BIPOLAR NEBULA S106

P. Pişmiş and I. Hasse

Instituto de Astronomía
Universidad Nacional Autónoma de México

Received 1980 March 31

RESUMEN

Se han determinado velocidades radiales por medio de interferometría Fabry-Pérot fotográfica, dentro y alrededor de la región bipolar pequeña (1 × 3 minutos de arco), Sharpless 106. La velocidad promedio del lóbulo más brillante está desplazada hacia el rojo por 5 km s^{-1} con respecto a su vecindad de brillo tenue. Esto probablemente indica que se está observando la parte de frente de una cáscara gruesa en expansión con opacidad interna alta. Se señala que las velocidades radiales de líneas en radio frecuencias muestran dos picos desplazados relativamente por ≅ 4 km s^{-1}, lo cual es consistente con el hecho que el objeto está asociado con una nube molecular, en particular de CO, la cual puede también estar expandiéndose. Una distancia cinemática en la longitud de S106 (74°.6) no es confiable. Se arguye que si se la estima por datos de radio, puede ser algo más confiable. Creemos que la distancia de S106 es menor que 1 kpc, más cerca a 600 pc, estando así de acuerdo con la sugerencia de Eiroa *et al.* (1979) basada en una argumentación física sobre la fuente de ionización de S106.

ABSTRACT

We have determined radial velocities by photographic Fabry-Pérot interferometry, at 236 points in and around the small (1 × 3 arcmin) bipolar H II region Sharpless 106. The average velocity of the brighter lobe is blue shifted by 5 km s^{-1} with respect to the fainter surroundings. This probably indicates that one is observing the front side of an expanding thick shell with high internal opacity. It is pointed out that radial velocities from radio frequencies show two peaks displaced by ≅ 4 km s^{-1}. This is consistent with the fact that the object is associated with a molecular, in particular a CO cloud, which may also be expanding. A kinematic distance at the longitude of S106 (74°.6) will not be too reliable. We argue that if any, it will be more reliable if estimated from radio data. We believe the distance of S106 to be less than 1 kpc, more nearly 600 pc, in agreement with the suggestion of Eiroa *et al.* (1979) based on physical arguments on the ionization source of S106.

Key words: **H II REGIONS – INTERFEROMETRY – RADIAL VELOCITY.**

I. INTRODUCTION

Sharpless 106 ($\alpha = 20^h25^m.6, \delta = +37° 14', 1950$) is a bright, small nebula with two components, "lobes", arranged in a bipolar configuration. The overall dimensions are 1 by 3 arc minutes. It was discovered by Minkowski (1946) on Palomar Schmidt plates, hence the alternative designation M1-99[1] (also G 76.4, −0.6 and CRL 2584).

1. This object is referred to as M1-19 by some authors. In fact it is number 19 in Table 2, the list of peculiar emission nebulae, and number 99 if the numbering continues from Table 1 (both from Minkowski 1946).

Several investigations carried out in the past few years have provided evidence that S106 has the characteristics of a young object; a number of infrared point sources have been identified in the region (Sharpless *et al.* 1977; Pipher *et al.* 1976). A photographic infrared study of the area is carried out by Eiroa *et al.* (1979). The contour map at λ6 cm emission of Israel and Felli (1978) has revealed three components at the densest borders of the lobes facing one another. There is general agreement in the position of these and the infrared sources reported by Pipher *et al.* (1976) and Eiroa *et al.* (1979). Continuum emission at 5 GHz (Kazès *et al.*, 1977) and at 10.5 GHz (Viner *et al.* 1976) has also been

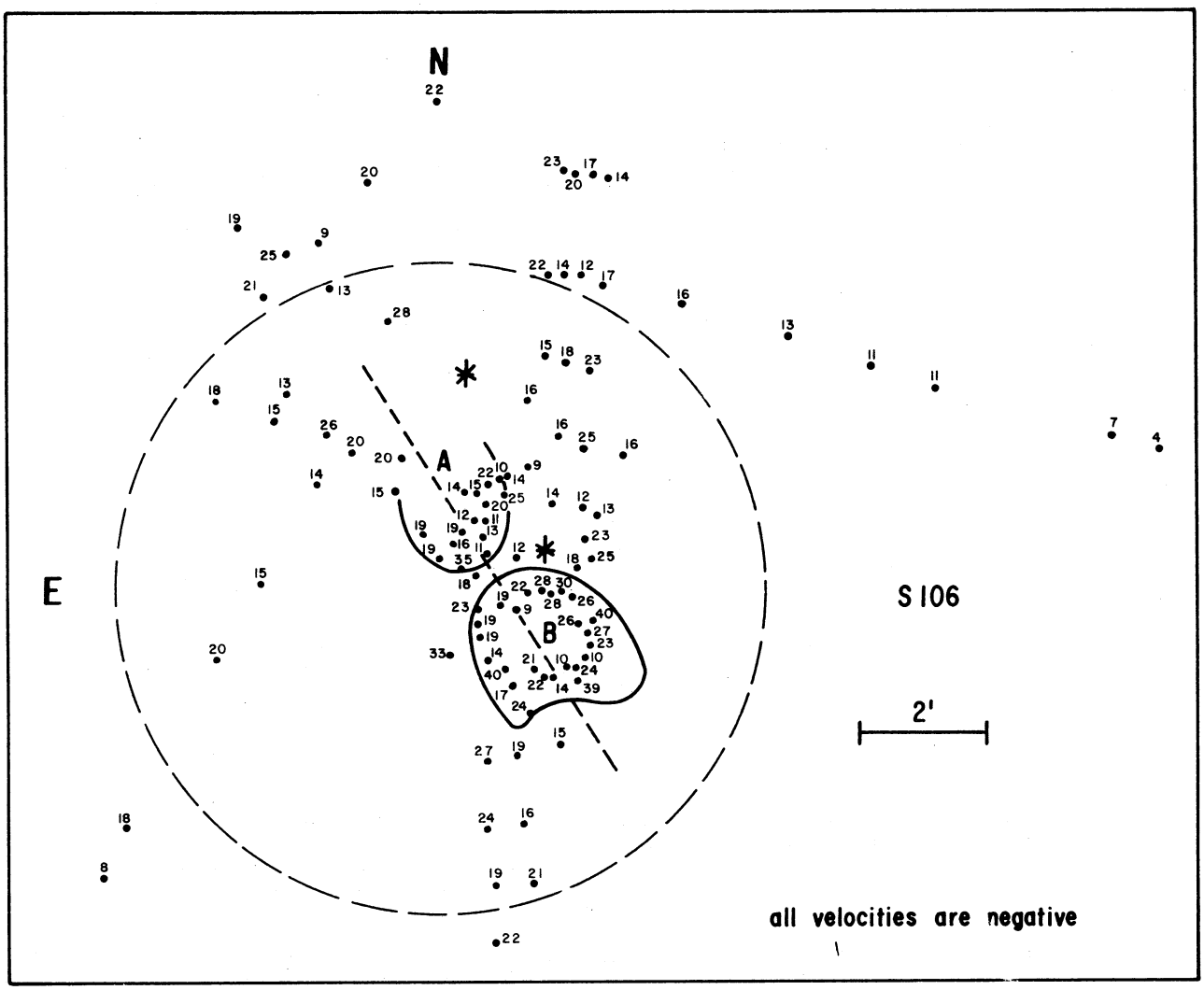

Fig. 2. Plot of 100 heliocentric radial velocities obtained from five interferograms on and around the H II region Sharpless 106. To minimize the congestion in the figure we have indicated the velocities in km s^{-1} without regard to sign; all velocities are negative. Our data have yielded 136 additional velocity points farther out to the west of S106; these fall outside the area covered by the figure. The different sub-regions are sketched by continuous lines (Maucherat's) and by dashed lines (ours).

reported. Detected also are the radio recombination lines H85α by Viner *et al.* (1976) H109α and H138β by Kazès *et al.* (1977) who have also studied the HI 21-cm line. According to Lucas *et al.* (1978) an extended molecular cloud is associated with S106. The same molecular cloud is also mapped with the ammonia molecule by Little *et al.* (1979).

In the optical region, Maucherat (1975) has discussed the velocity field of S106 from Fabry-Pérot interferometry. Deharveng and Maucherat (1978) from monochromatic photographs find a uniform, rather low excitation over S106 and quite a high electron density. We report here on the radial velocity obtained from photographic Fabry-Pérot interferometry covering S106 and its surroundings and, pending a detailed treatment, also present two high resolution spectra representative of the northern and sourthern lobes, respectively.

II. THE OBSERVATIONS

On Palomar Sky Survey Prints S106 appears as an isolated H II region but on our image-tube Hα direct

photographs (a sample is reproduced in Figure 1, Plate 1) as well as on our interferograms the tenuous extensions covering nearly 30 arcmin appear to be associated with the nebula. Five interferograms were selected as the best among several obtained in the region (exposure times about 15 min). These interferograms overlap slightly so that the region studied covers S106 and the surroundings within an area of 23 X 28 arc minutes.

Three of the interferograms are taken using an étalon with interorder separation of 283 km s^{-1} and the remaining two using an étalon with an interorder separation of 190 km s^{-1}. In all cases a 10 Å halfwidth interference filter is employed to isolate the Hα line. Further details of the equipment are given in earlier publications (see for example Pişmiş and Hasse 1976). There does not seem to be any systematic difference between the velocities from the different étalons. The interferograms are measured visually using the Mann Comparator of the NASA Johnson Space Center and the reductions carried out following the scheme given by Courtès (1960). 236 velocity points are obtained from the five interferograms; 100 of the velocity points which are in the immediate neighborhood of S106 are mapped in Figure 2. We have not deemed it relevant to display the outer 136 radial velocities although we shall comment briefly on them later. All velocities should be taken with a negative sign. To enable a direct comparison with previous studies, the outline of the two components of S106 is also drawn on that figure, following the sketch given by Maucherat (1975). Further subdivisions introduced by us are indicated by dashed lines. The same sketch appears again in Figure 3 where the numbers stand for the average velocities in the different sub-regions (all velocities are heliocentric unless specified otherwise).

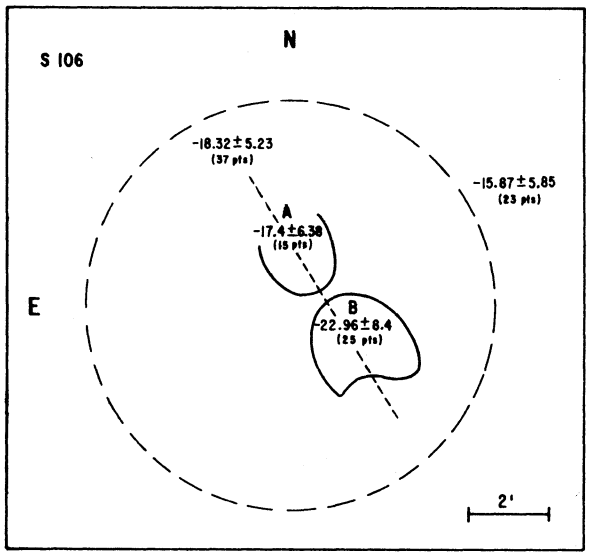

Fig. 3. The sketches are the same as in Figure 3. The numbers indicate average velocities with standard deviations and the number of velocity points falling in each sub-region.

It is clear from Figure 2 that the radial velocities within S106 proper cover a wide range of values. The only other known optical velocity field, that of Maucherat (1975), also shows this peculiarity. But unlike Maucherat we have been unable to detect a splitting of interference rings on any of our interferograms; perhaps the rather long exposure and the small scale, 1.5 arcmin mm^{-1}, of our interferograms has concealed a doubling of the pattern.

In Figure 2 the dashed line through the middle of the northern and southern lobes (hereafter we refer to these features as A and B following earlier designations) is roughly an axis of symmetry for S106 and is parallel to what is believed to be the axis of rotation of the surrounding extended CO cloud (Lucas *et al.* 1978). Individual velocity points do not reveal a significant trend within the lobes; therefore we consider only the averages.

Average radial velocities at the east and west sections of lobe B give -21.1 km s^{-1} (11 pts) and -24.4 km s^{-1} (14 pts) respectively while the averages corresponding to Maucherat's values are -31.1 km s^{-1} (7 pts) and -17.9 km s^{-1} (10 pts) respectively. Thus with the presently available data there seems to be no indication of a rotation of the optical nebula. The overall velocity of B is -23.0 ± 8.4 km s^{-1} (25 pts). (Maucherat's average value is -24.5 km s^{-1}). The average velocity of A is -17.4 ± 6.4 km s^{-1} (15) (all errors are rms) and the mean line of sight motion of the surrounding faint nebula is -18.3 ± 5.2 km s^{-1} (37 pts). The radial velocity of A is thus quite comparable to that of the surrounding tenuous nebula. Assuming that A and B are physically related and are moving together –a very plausible assumption– a resultant negative velocity for B with respect to A, as well as with respect to the surrounding nebula, is of the order of 5 km s^{-1}. This may mean that we are observing preferentially the near side of an expanding nebula of which the far side is mostly unobservable due to the high density of internebular dust. The high degree of obscuration of this area particularly of B is consistent with results obtained from several infrared studies (Pipher *et al.* 1976; Sibille *et al.* 1975; Eiroa *et al.* 1979).

An expansion of 5 km s^{-1} is an average value and is expected to be much smaller than the real expansion velocity. Maucherat (1975) suggests an expansion of 36 km s^{-1} based on the doubling of interference rings at 2

TABLE 1

RADIAL VELOCITIES OF S106 FROM OPTICAL AND RADIO LINES

Line	Radial velocity km s^{-1} (LSR)	Source
Hα	− 3.2	Georgelin *et al.* (1973)
Hα	− 9	Maucherat (1975)
Hα	− 1.5	This paper
H85α	+ 2.9	Viner *et al.* (1976)
H109α	+ 5.6	Reifenstein *et al.* (1970)
H109α	+ 3.5	Kazès *et al.* (1977)
137β	+ 3.5	Kazès *et al.* (1977)

points in lobe B. This value is probably larger than the real one.

Radial velocities (LSR) determined to date from optical and radio recombination lines for S106 are listed in Table 1 with pertinent references. We note that our LSR velocity, −1.5 km s^{-1}, corresponds to −18.3 km s^{-1}, the average heliocentric velocity of the surrounding diffuse nebula as indicated in Figure 3. We believe our radial velocity to be a reliable one not only because it is based on a larger number of points (100) compared to Maucherat's but also because we have been able to isolate the overall velocity field from local effects such as internal motions or a possible expansion of lobe B.

As Table 1 clearly shows, the optical LSR velocities of S106 are negative while those of radio recombination lines are positive. The range covered is around 14 km s^{-1}. We note however, that the profiles of the radio recombination lines, whenever given, in particular that of H109α, show two peaks corresponding to positive and negative velocities. The velocities listed in Table 1 are probably averages, determined by fitting a single Gaussian to the profiles. Unfortunately the published tracings (Kazès *et al.* 1977) are on too small a scale to enable a reliable evaluation of the two components separately. It would be interesting to know whether the H85α line profile also shows two peaks but no profiles are published by Viner *et al.* (1976) to know this.

A negative component is also present in the 21-cm line; Kazès *et al.* (1977) state that their H I profile shows two prominent features at + 3 and −6 km s^{-1} respectively but only the + 3 km s^{-1} component is listed by Israel and Felli (1978). Emission lines from molecules such as CO, HCO^+, HCN, H_2CO and the absorption line of H_2CO also favor negative velocities at the peak of the prominent profile which in all cases is quite wide (Lucas *et al.* 1978).

The following are our rough estimates from published profiles (Lucas *et al.* 1978) of the velocities which will be mentioned only and not tabulated. The CO line profile shows a prominent peak around −1 km s^{-1} (LSR) and a slight indication of a maximum at + 4 km s^{-1}. HCO^+ has a prominent maximum at −1 km s^{-1}. H_2CO shows only one wide profile around −2 km s^{-1}. The H_2CO absorption minimum corresponds to −1.5 km s^{-1} and no component at positive velocities can be detected. Two OH absorption lines at 1665 and 1667 MHz respectively show a pronounced minimum between −1 and −2 km s^{-1} and a very slight indication of a second minimum around + 4 km s^{-1}.

The difference between the two velocity components is quite small on the average not exceeding 4 km s^{-1}, and is comparable to the velocity difference between the east and west edges of the CO cloud where S106 is embedded (Lucas *et al.* 1978); as mentioned earlier the difference is interpreted as due to the rotation of the CO cloud. A slight variation from east to west in the radial velocities of the molecular cloud is also shown by the observations of the ammonia molecule (Little *et al.* 1979). The velocities are in the range −1.3 to −2.1 km s^{-1}. Summarizing we may state that:

1) A negative velocity in the range −1 to −2 km s^{-1} is rather well established for the region of S106 from all wavelengths.

2) An indication of a positive radial velocity is: nonexistent for the Hα line, mildly present for molecular emission and absorption lines and definitely present for the recombination lines H109α, H137β, and the 21-cm HI line. The presently available data do not lead to a firm conclusion whether the positive and negative velocities are manifestations of motions within the same cloud (such as an expansion or a contraction of a shell) or that they represent two separate regions projected along the line of sight).

It is worth mentioning that our interferograms have shown distinctly measurable Hα inteference rings up to a distance of 20 arcmin to the west of S106 (we have no data towards the east); within this distance and beyond the area covered by Figure 2 or 3, we have obtained 136 velocity points in two sample regions. These are sectors of about 30° centered on S106, one towards the northwest and the other towards the southwest. As mentioned earlier we have not given a plot of these velocities; instead we give their average velocity −15.8 ± 6.6 km s^{-1}. We note that this is comparable to the average found outside the circle in Figure 3. There is indication, therefore, that this extended H II region is spatially related to S106 and that the whole complex may cover at least half a degree.

III. THE DISTANCE OF S106

A photometric distance for S106 cannot as yet be evaluated since the excitation source is not firmly established nor can the kinematic distance be satisfactorily estimated. First because velocity determinations from different wavelengths and sources give discrepant values (cf. Table 1); second, peculiar and random motions, at the longitude of this objet (74°.6) may compete with or be even larger than the small differential rotation effect and finally the differential rotation effect alone is a rather unreliable measure of the distance at these galactic longitudes. To illustrate the latter we have calculated the kinematic distance corresponding to a set of V_{LSR} for $\ell = 74°.6$. Table 2 gives the distances. Note that for negative velocities the distance is unambiguous but for positive velocities there are two possible values. The situation will be similar in the fourth galactic quadrant at a direction close to $\ell = 270°$.

It may be argued that optical velocities may not represent the motion of the complex S106 since we may be observing the near side hence the negative velocities of a possibly expanding region, a thick shell, with high internal opacity. In fact the extended 30 arcmin dense molecular cloud around S106 (Lucas *et al.* 1978) suggests that considerable obscuration may be associated with it. However, the radio data show also negative velocities along with positive ones.

We have reason to believe that the velocity closest to the real value of the centroid of the S106 complex is given by the radio recombination lines listed in Table 1, since these values represent evidently the averages over the negative and positive (presumably the average of the approaching and receding velocities) peaks of the profiles discussed above. We take therefore the average over the four independent determinations of velocity from radio recombination lines at face value, $V_{LSR} = +3.8$ km s^{-1}, to represent the velocity of the system of S106. Using the Schmidt rotation curve (Schmidt 1965) we obtain 2 values for the distance namely 0.58 and 4.12 kpc respectively (for R_0 = 10 kpc). As we shall see later, 0.58 kpc agrees with the distance for S106 suggested by Eiroa *et al.* (1979) from independent arguments.

For the sake of completeness we give distances obtained from other average velocities: our optical heliocentric velocity for S106 complex adopted as -18.3 km s^{-1}, corresponding to $V_{LSR} = -1.5$ km s^{-1}, gives a distance of 4.86 kpc and the average over all optical velocities (Table 1) yields a distance of 5.2 kpc.

Although more reliable determinations and a thorough discussion of the radial velocity field from the optical as well as the radio range may be rewarding it seems to us doubtful whether one can locate unambiguously from kinematical data alone the sources in which the observed Doppler shifts arise.

TABLE 2

KINEMATIC DISTANCES FOR ASSUMED V_{LSR} AS INDICATED

V_{LSR} (km s^{-1})	R (kpc)	r_1 (kpc)	r_2 (kpc)
− 9	10.28	5.70	....
− 7	10.24	5.57	....
− 5	10.17	5.34	....
− 3	10.06	4.94	....
− 1	10.02	4.78	....
+ 1	9.98	4.61	0.09
+ 3	9.91	4.28	0.42
+ 5	9.81	3.68	1.02
+ 7	9.72	2.37	2.33

IV. THE SOURCE OF IONIZATION

Within the two lobes no star-like objects are known from direct observation responsible for the ionization of S106. Calvet and Cohen (1978) have obtained optical spectra of a compact knot, in lobe B, associated with an infrared source (source 1 of Pipher *et al.* 1976). Along with emission lines they find a very red continuum which is interpreted as dust scattered light from a hot star embedded in the knot. From scanner narrow-band color indices they estimate A_v to be 8.2 ± 1.3 magnitudes. They suggest further that an O9V star presumably within the knot is not expected to be capable of providing sufficient ultraviolet photons to account for the complex of infrared and radio sources associated with S106. This conclusion is however dependent on the distance of S106 usually adopted to be not less than 2.5 kpc although this is not mentioned explicitly by Calvet and Cohen (1978).

Four compact infrared sources were detected by Pipher *et al.* (1976) at wavelengths 12.6μ and 3.5μ. Their source 3 which lies halfway between the north and south lobes agrees in position with the source which Sibille *et al.* (1975) have detected in the range 1.25μ to 3.4μ. In the photograph around 8000 Å by Pipher *et al.* (1976) source 3 appears rather fuzzy; these authors suggest that the object is an incipient trapezium system and is the ionization source of the S106 complex. The existence of such a trapezium between the components of S106 was tacitly accepted until lately.

Eiroa *et al.* (1979) have recently provided strong

evidence that source 3 is not a trapezium system. Their infrared photographs at 0.92μ (I) show clearly the image of a single star. This star does not appear on their photograph at 0.70μ (R). It is therefore concluded that a hot star which may be the ionization source of S106, is embedded in an obscuring flat disk between the lobes.

Eiroa *et al.* go on to discuss the infrared spectrum of source 3 using infrared fluxes from other authors to which they add their R and I flux values and conclude that the best fit to the observed energy spectrum is obtained for a combination of the following parameters for the ionization source; spectral type of the star, B0V to O9V; extinction by the flat disk where the star is embedded, $A_V = 20.8$ mag; and distance, around 500 pc. The value of the extinction is indeed quite high but the overall region is one of high extinction. Independent estimates of A_v for sources 1 and 2 of Pipher *et al.* located near the southern and northern borders of the dust lane, yield $A_V = 5$ mag for source 1 and $A = 11$ mag for source 2. It may be of interest to recall that a distance of 0.58 kpc is obtained kinematically using $V_{LSR} = +3.8$ km s^{-1}, the average velocity of the radio recombination lines of Table 1, a velocity which as argued above is likely to represent the overall motions of the S106 complex. This distance of 0.58 kpc. happens to agree with that suggested by Eiroa *et al.* (1979).

V. THE SPECTRA OF S106 A AND B

Two high resolution spectra were obtained of S106 A and S106 B respectively at the region of Hα with the multichannel system attached to the 1-meter reflector at the National Observatory in Tonantzintla. These spectra are reproduced in Figure 4. A quantitative treatment of the spectra will be done later when more spectra are obtained. Attention is called at this stage to the strength of the [N II] λ 6584 line and the [S II] $\lambda\lambda$ 6717 and 6731 lines with respect to Hα. The strong [N II] and [S II] lines indicate that the ionization degree in S106 is rather low. As to the ratio of the peak intensities of [S II] lines, it is 0.55 ± 0.05 and 0.66 ± 0.07 respectively for S106A and S106B. If the slight difference

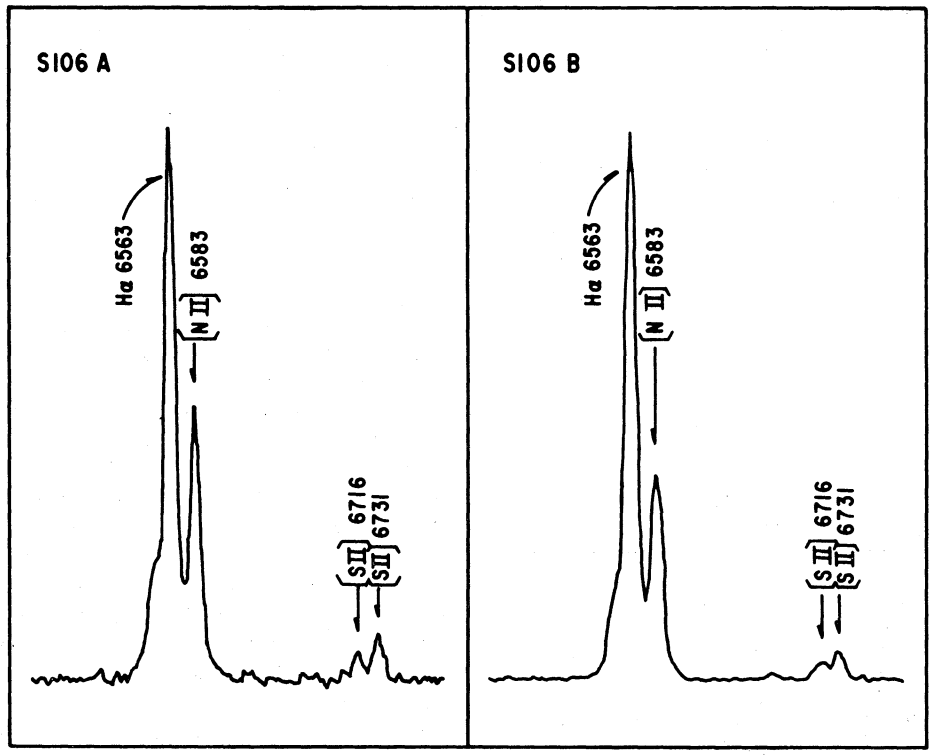

Fig. 4. Tracings of the spectra of the northern (A) and southern (B) lobes of S106 with a Cassegrain spectrograph and a multichannel detector attached to the 1-meter telescope of the Observatorio Astronómico Nacional at Tonantzintla. Rest wavelengths are marked in the figures.

in these ratios could be trusted, based on the relation ratio of the intensities, I (λ 6716)/I(λ 6731) of [S II] versus $N_e\ T^{-½}$ (see for example Osterbrock 1974) this would mean the $N_e\ T^{-½}$ is higher in the northern lobe than in the southern one. If the temperature were the same in both lobes the northern lobe would have the higher electron density. However, Glushkov and Karyagina (1971) determine the ratio of the intensities of the [S II] doublet, I(λ6717)/I(λ6731) in S106 as 0.68 for the northern and 0.78 for the southern lobe. Based on these values their estimate of the electron densities yield 5600 cm^{-3} and 8500 cm^{-3} in the northern and southern lobes respectively.

VI. CONCLUSION

We have discussed the velocity field obtained from five interferograms covering an area of roughly 23 by 28 arc minutes of the small H II region, S106 and the tenuous nebula around it. We have obtained a systematic LSR velocity of −1.5 km s^{-1} for the complex. The northern lobe of S106 has a velocity comparable to the surrounding faint extensions while the southern lobe has an excess negative velocity of about 5 km s^{-1} indicating probably that we are observing the near side of an expanding structure with high internal obscuration.

The existence of double peaks of the radio recombination lines and similar double values of the molecular lines are stressed. These are discussed in the context of the predominance of negative optical velocities from our FP interferometry and from earlier FP results by Maucherat. A plausible explanation is that one is observing in the radio range the near and far sides of an expanding larger cloud perhaps a thick shell surrounding S106 with rather high internal extinction while optically one observes only the near side. The overall region around S106 is one of high extinction.

The distance of the complex is probably less than 1 kpc, more nearly 600 parsec. The dimensions of the nebula would then be 0.18 X0.24 pc. At this distance, closer than assumed so far, the ionization source may be a single O9V star between the two lobes as argued by Eiroa *et al.* (1979) and not a trapezium. S106 thus appears to satisfy one more of the criteria of a bipolar nebula.

The authors wish to thank M.A. Moreno and A. Quintero who have obtained the interferograms.P.P. acknowledges with thanks the facilities offered her at the NASA Johnson Space Center.

REFERENCES

Calvet, N. and Cohen, M. 1978, *M.N.R.A.S.*, **182**, 687.
Courtès, G. 1960, Ann. d'Ap., **23**, 115.
Deharveng, L. and Maucherat, M. 1978, *Astr. and Ap.*, **70**, 19.
Eiroa, C., Elsässer, H., and Lahulla, J.F. 1979, *Astr. and Ap.*, **74**, 89.
Georgelin, Y.M., Georgelin, Y.P. and Roux, S. 1973, *Astr. and Ap.*, **25**, 337.
Glushkov, Yu. I. and Karyagina, S.V. 1971, *Astr. Tsirk.*, **632**, 3.
Israel, F.P. and Felli, M. 1978, *Astr. and Ap.*, **63**, 325.
Kazès, I., Walmsley, C.M., and Churchwell, E. 1977, *Astr. and Ap.*, **60**, 293.
Little, L.T., McDonald, G.H., Riley, P.W., Matheson, D.N. 1979, *M.N.R.A.S.*, **188**, 429.
Lucas, R., Le Squeren, A.M., Kazès, I., and Encrenaz, P.J. 1978, *Astr. and Ap.*, **66**, 155.
Maucherat, Y.J. 1975, *Astr. and Ap.*, **45**, 193.
Minkowski, R. 1946, *Pub. A.S.P.*, **58**, 305.
Osterbrock, D.E. 1974, *Astrophysics of Gaseous Nebulae*, (Freeman and Co.).
Pipher, J.L., Sharpless, S., Savedoff, M.P., Kerridge, S.J., Krassner, J., Schurmann, S., Soifer, B.T., and Merrill, K.M. 1976, *Astr. and Ap.*, **51**, 255.
Pişmiş P. and Hasse, I. 1976, *Ap. and Space Sci.*, **45**, 79.
Reifenstein III, E.C., Wilson, T.L., and Burke, B.F. 1970, *Astr. and Ap.*, **4**, 357.
Sharpless, S., Pipher, J.L., Savedoff, M.P., and Schurmann, S. 1977, *Rev. Mexicana Astron. Astrof*, **3**, 167.
Sibille, F., Bergeat, J., Lunel, M., and Kandel, R. 1975, *Astr. and Ap.*, **40**, 441.
Viner, M.R., Clarke, J.N., and Hughes, V.A. 1976, *A. J.*, **81**, 512.

Paris Pişmiş and Ilse Hasse: Instituto de Astronomía, UNAM, Apartado Postal 70-264, México 20, D.F., México